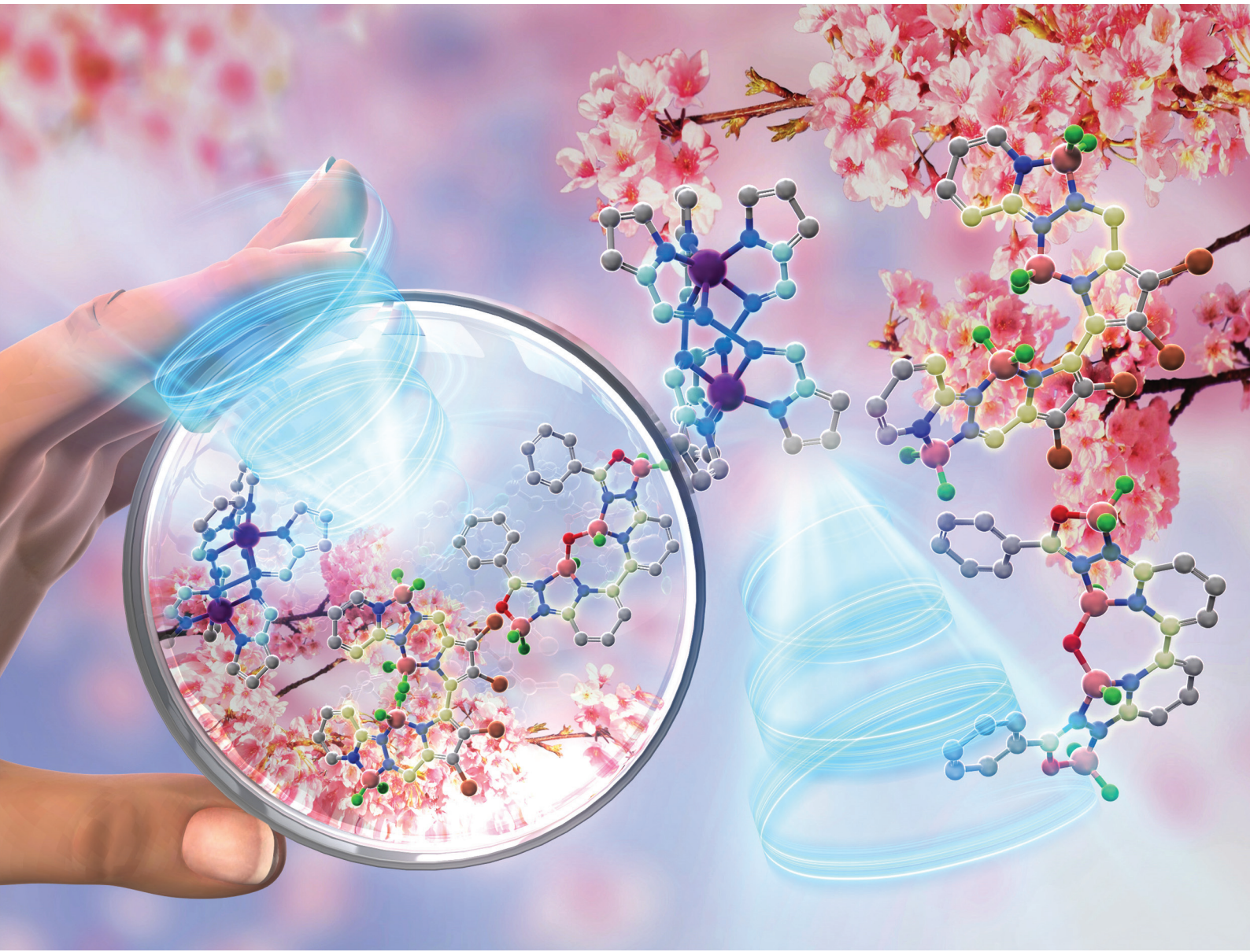


# Dalton Transactions

An international journal of inorganic chemistry

[rsc.li/dalton](http://rsc.li/dalton)



ISSN 1477-9226

## FRONTIER

Toshikazu Ono and Yousuke Ooyama  
Axial and helical chirality in multinuclear group 13  
complexes: pathways to functional optical materials



Cite this: *Dalton Trans.*, 2025, **54**, 6361

Received 29th January 2025,  
Accepted 14th March 2025  
DOI: 10.1039/d5dt00230c  
[rsc.li/dalton](http://rsc.li/dalton)

## Axial and helical chirality in multinuclear group 13 complexes: pathways to functional optical materials

Toshikazu Ono <sup>\*a</sup> and Yousuke Ooyama <sup>\*b</sup>

Main-group element complexes have emerged as promising functional dyes owing to their unique photo-physical properties and potential applications in sensors, luminescent devices, and photocatalysis. Among these, multinuclear main-group complexes that incorporate multiple elements within a single ligand have garnered significant attention, particularly for their ability to exhibit chirality with optical functions. Axial and helical chirality, resulting from unique coordination geometries, represent a critical frontier in the design of functional materials. These complexes enable diverse functionalities, including circular dichroism and circularly polarized luminescence. This Frontier article highlights recent advances in the synthesis of multinuclear main-group element complexes with chirality, focusing on their structural uniqueness and photochemical characteristics. Particular emphasis is placed on group 13 element complexes, including boron(III), aluminum(III), gallium(III), and indium(III), which exhibited unique chiral properties and photo-physical behaviors. Key topics include the design strategies for chiral multinuclear frameworks, their photophysical properties, and their integration into advanced functional materials.

## Introduction

Chirality plays a central role in the design and development of advanced functional materials, particularly for optical applications. The ability to control and manipulate chiral structures has driven significant progress in areas such as chiral sensing, enantioselective catalysis, and the generation of circular dichroism (CD) and circularly polarized luminescence (CPL). Recently, multinuclear main-group element complexes, which integrate multiple elements into a single framework, have emerged as promising candidates for generating both axial and helical chirality. These complexes offer distinct advantages over traditional metal-centered systems, including greater flexibility, synthetic accessibility, and the ability to achieve chiral properties derived from the ligands rather than the central metal atoms.

Axial chirality in these complexes typically arises from steric hindrance due to high inter-ligand rotational barriers that prevent free rotation around specific bonds, thereby stabilizing the chiral configuration.<sup>1</sup> This phenomenon is commonly

observed in organic molecules as well as in coordination complexes. In contrast, helical chirality occurs in coordination compounds with higher coordination numbers, such as six-coordination geometries, where the structure induces twisting of the ligand framework, resulting in the formation of a helical arrangement. This feature is particularly pronounced in multinuclear complexes, where the increased number of coordinating ligands facilitates the formation of stable helical chirality without racemization, opening avenues to chiral configurations with significant photophysical properties. The unique structure–property relationships exhibited by axially and helically chiral multinuclear main-group complexes make them highly attractive for applications in the development of functional optical materials.<sup>2–4</sup> Introducing chirality into these frameworks has been shown to enhance their redox activity, optical properties, and, in some cases, thermal stability, further expanding their potential for use in advanced materials. In addition, designing chiral complexes with tailored functionalities enables the creation of materials with improved performance for various optoelectronic applications, including sensors, catalysis, and CPL-based devices.

Owing to these attributes, chiral multinuclear main-group element complexes hold immense potential as next-generation materials for diverse applications. This Frontier article focuses on the design and synthesis of such complexes, particularly those based on group 13 elements–boron, aluminum, gallium, and indium–emphasizing their chiral characteristics,

<sup>a</sup>Department of Applied Chemistry, Graduate School of Engineering, Center for Molecular Systems (CMS), Kyushu University, 744 Motooka, Nishi-ku, Fukuoka, 819-0395, Japan. E-mail: [tono@mail.cstm.kyushu-u.ac.jp](mailto:tono@mail.cstm.kyushu-u.ac.jp)

<sup>b</sup>Applied Chemistry Program, Graduate School of Advanced Science and Engineering, Hiroshima University, 1-4-1 Kagamiyama, Higashihiroshima, 739-8527, Japan. E-mail: [yooyama@hiroshima-u.ac.jp](mailto:yooyama@hiroshima-u.ac.jp)

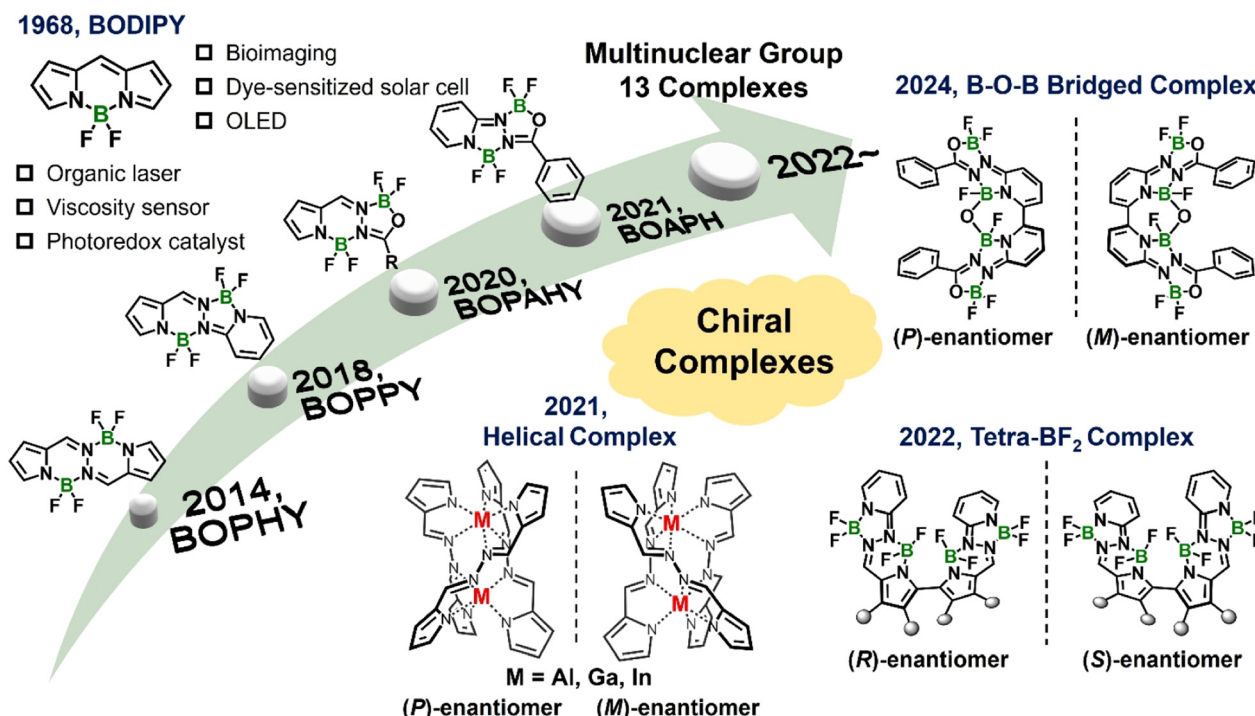


Fig. 1 Structures of achiral boron complexes and recently developed multinuclear group 13 complexes with axial/helical chirality.

photophysical properties, and functional integration into materials. To achieve this, we explore design strategies inspired by relatively simple multidentate ligand structures, such as luminescent boron-based dinuclear complexes (BOPHY,<sup>5</sup> BOPPY,<sup>6</sup> BOPAHY,<sup>7</sup> BOAPH,<sup>8</sup> *etc.*), which have been frequently reported in recent years.<sup>9</sup> We investigate methods to create new frameworks by dimerizing these boron complexes and further substituting them with other group 13 elements (Fig. 1). Specific topics include the strategies for introducing chirality into multinuclear frameworks, the influence of chirality on photophysical behaviors, and the potential applications of these complexes in CD and CPL.

## Multinuclear boron complexes with axial chirality

Boron-dipyrromethene (BODIPY) is among the most well-known boron complexes for creating chiral boron complexes. While mononuclear BODIPY-based complexes have been extensively studied, recent advancements have shifted focus to multinuclear derivatives, including dinuclear complexes, which demonstrate enhanced structural diversity and unique optical properties (Fig. 1).<sup>9</sup> These multinuclear systems display fascinating coordination geometries, where the interplay between multiple boron centers and their ligands significantly influences their overall properties. Recent studies have uncovered novel coordination modes that enable axial/helical chirality through asymmetric ligand arrangements, emphasizing the

importance of precise molecular design in achieving desirable chiroptical properties, such as strong CD signals.<sup>10</sup> These characteristics make such complexes highly relevant for applications in chiral sensing and optoelectronics. The creation of chiroptically active boron-containing systems faced challenges due to the predominantly planar and achiral nature of most boron complexes. Current strategies for preparing chiroptical boron-containing chromophores often rely on BODIPY skeletons incorporating chiral perturbations. These include chiral substituents combined with boron difluoride ( $\text{BF}_2$ ) configurations, boron-bridged orthogonal combination fluorophore-chiral element combinations, or the introduction of boron as a chiral center through tetra-coordination-induced asymmetry.<sup>10,11</sup> However, researchers continue to explore diverse chiral boron complexes beyond BODIPY derivatives.

Studies on other mononuclear and multinuclear boron complex derivatives *via* molecular engineering shows potential to surpass existing works on BODIPY derivatives. Recent efforts have focused on creating novel photofunctional properties through the dimerization of these dinuclear boron complexes.<sup>12–17</sup> Several systematic studies have reported innovative multinuclear boron complexes containing tetra- $\text{BF}_2$  groups based on 2,2'-bipyrroles which have been widely used as precursors for porphycene synthesis (Fig. 2).<sup>18–21</sup> These “flag-hinge” complexes, synthesized using a one-pot method (Fig. 2a), demonstrated multicolor fluorescences, high quantum yields reaching 100%, large Stokes shifts, and CPLs induced by axial chirality, along with electrochemiluminescence and laser properties.<sup>17</sup> Structural analyses *via* X-ray



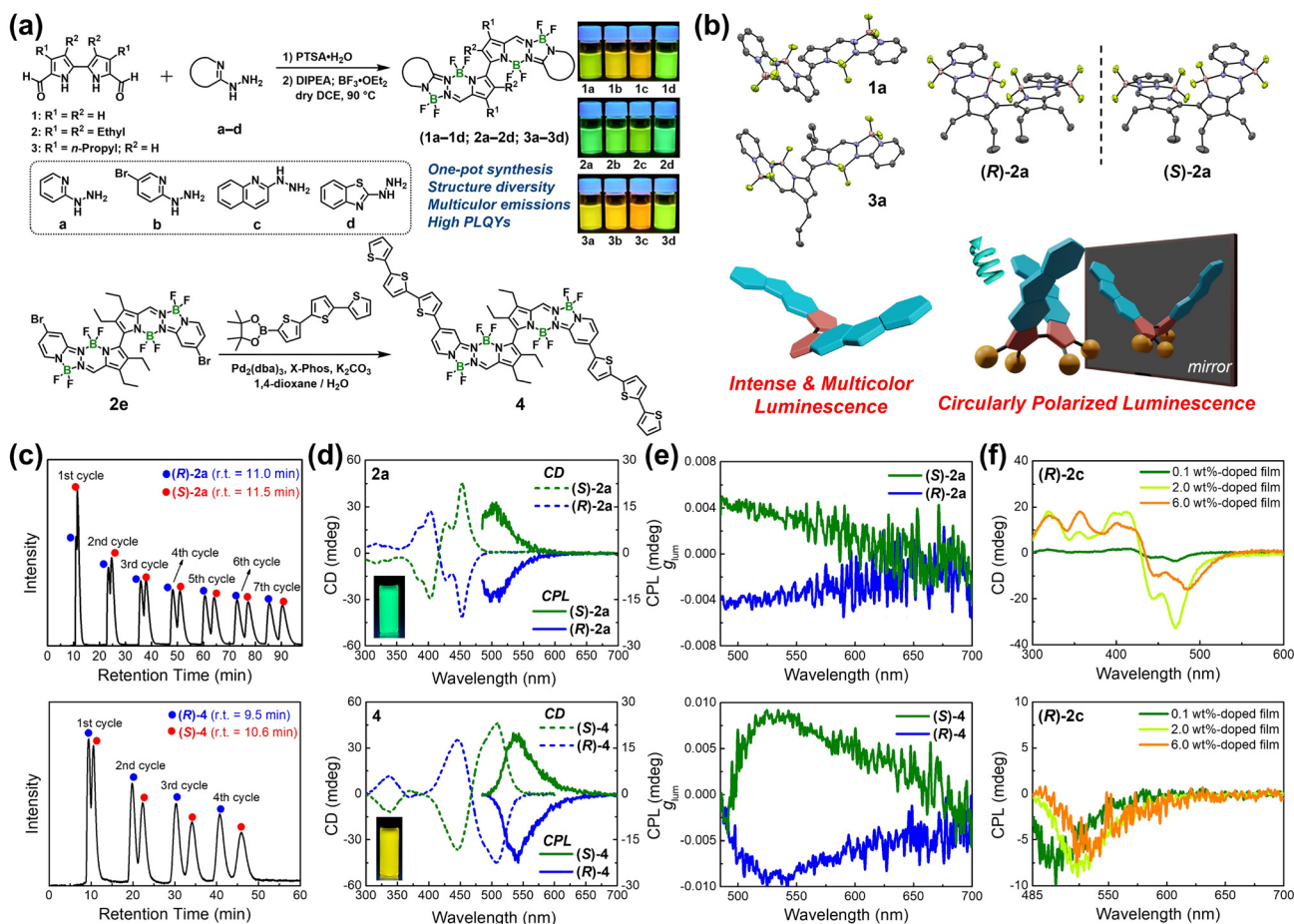


**Fig. 2** (a) Synthesis of multinuclear boron complexes with axial chirality. Reproduced with permission from ref. 13 copyright (2022) Wiley and ref. 15 copyright (2023) Royal Society of Chemistry. (b) X-ray single crystal structures of **1a**, **2a**, and **3a** with schematic figures of “flag-hinge” complexes including axial chirality. Ellipsoids are set at 50% probability. Reproduced with permission from ref. 13 copyright (2022) Wiley. (c) Optical resolutions for the separation of enantiomers of **2a** and **4**. Reproduced with permission from ref. 13 copyright (2022) Wiley and ref. 15 copyright (2023) Royal Society of Chemistry. (d and e) Chiroptical properties (CD, CPL, and  $g_{\text{lum}}$  spectra) of enantiomers of **2a** and **4** in toluene. Reproduced with permission from ref. 13 copyright (2022) Wiley and ref. 15 copyright (2023) Royal Society of Chemistry. (f) CD and CPL spectra of **(R)-2c**-doped poly (methyl methacrylate) films. Reproduced with permission from ref. 13 copyright (2022) Wiley.

crystallography and computational calculations reveal a bent molecular conformation, like a “flag-hinge” (Fig. 2b). The complexation of various synthesized hydrazone Schiff ligand moieties with  $\text{BF}_2$  group alters the electronic state and  $\pi$ -conjugation degree of the whole molecule, attributing to excellent photophysical properties. Axial chirality is induced by restricting rotation around the bipyrrole axis through steric hindrance when bulky substituents are introduced on the bipyrrole precursor, enabling the isolation of (R)- and (S)-enantiomers using chiral column chromatography (Fig. 2b and c). These enantiomers exhibit strong CD and CPL responses, with luminescence dissymmetry factors ( $g_{\text{lum}}$ ) in the typical range of  $10^{-3}$  order (Fig. 2d and e). By adjusting molecular aggregation states, CPL activity remains robust, and chiral enantiomer-doped polymer films exhibit color-tunable luminescence, ranging from green and yellow to orange (Fig. 2f). By leveraging axial chirality and aggregation-induced effects, these multinuclear boron complexes are promising

candidates for high-performance chiral photofunctional materials, offering for innovations in optoelectronics, bio-imaging, and information storage. Furthermore, tunable CPL emissions from green to orange with high  $g_{\text{lum}}$  values in solution and solid state have been achieved by designing new tetra- $\text{BF}_2$  complexes modified by terthiophene moieties at specific positions *via* the Suzuki–Miyaura coupling reaction (Fig. 2a).<sup>15</sup> Interestingly, complexes with terthiophenes substituted at the *para*-position relative to the pyridine moiety exhibit yellow fluorescence and CPL with a high  $g_{\text{lum}}$  value up to  $10^{-2}$  (Fig. 2d and e). These findings are attributed to the extended  $\pi$ -conjugation and improved intramolecular charge transfer (ICT) interactions *via* terthiophene modification. The highly luminescent multicolor CPLs achieved using emissive boron chromophores offer broad applications in CPL technology. These findings further highlight their potential for advanced chiroptical applications, including 3D displays, encryption, and sensors.

## Multinuclear boron complexes with helical chirality

Helical chirality in multinuclear boron complexes has attracted significant attention in recent years. Advances in this area have reported the synthesis of dinuclear boron complexes exhibiting twisted frameworks, which lead to well-defined helical chirality. The structural diversity of these multinuclear systems arises from their unique coordination environments, which are often stabilized by strong intermolecular interactions and stereoelectronic effects. These helically chiral boron complexes exhibit exceptional chiroptical properties, making them promising candidates for applications in advanced photonic materials and enantioselective catalysis.<sup>22</sup> This section explores their coordination geometries, design strategies, underscoring their potential for functional material development.

BODIPY derivatives have garnered considerable attention due to their remarkable spectroscopic properties. Similar to their axially chiral counterparts, helically chiral boron systems are often inspired by BODIPY frameworks. To achieve the chiroptical activity in achiral BODIPYs, typical approaches involve combining them with chiral fragments or introducing axial chirality. However, the resulting chiral boron complexes often display weak chiroptical responses which are attributed to small coupling between the chiral fragments and the light-emitting centers within the molecule.<sup>10,11,22</sup> In 2022, Lu and coworkers introduced a novel molecular design for helical dinuclear B–O–B bridged complexes based on  $\beta$ -isoindigo to achieve red to near-infrared (NIR) CPL with a  $g_{\text{lum}}$  value in a  $10^{-3}$ .<sup>23,24</sup> These efforts leverage modular synthesis and distorted helical structures attributed to enhanced  $\pi$ -extension and optimized dipole moments for high CPL performance, being promising candidates for next-generation photonic devices and biomedical tools, particularly in applications requiring high precision and efficiency in the NIR region. Actually, B–O–B bridged multinuclear complexes have traditionally focused on tetrapyrrole complexes with a porphyrinoid core,<sup>25–28</sup> with one notable exception based on BOPPY framework.<sup>29</sup> However, the chirality of this family and the construction of new B–O–B bridged complexes with chiroptical properties have been less explored. The helical structure observed in these complexes promoted us to imagine their chiroptical performance as revealed by extensively studied helicenes.<sup>30</sup> Beyond the aforementioned BODIPY analogs with a B–O–B bridge, we developed a groundbreaking system for simultaneously achieving two distinct multinuclear boron complexes: a flag-hinged tetra-BF<sub>2</sub> complex and a helical B–O–B bridged complex. These two complexes were accomplished by reacting 6,6'-dihydrazineyl-2,2'-bipyridine with various acyl chlorides, followed by BF<sub>3</sub>·OEt<sub>2</sub> complexation (Fig. 3a).<sup>16</sup> The tetra-BF<sub>2</sub> complexes adopted a flag-hinged structure with significant conformational flexibility around the bipyridine axis and exhibited blue to yellow-green fluorescence (Fig. 3b). Solvent-dependent fluorescence demonstrated ICT interactions

in these tetra-BF<sub>2</sub> complexes, as supported by DFT and TD-DFT calculations. Notably, the dimethylaminobenzene-substituted tetra-BF<sub>2</sub> complex transitioned from yellow to blue emission under acidic conditions due to the inhibition of ICT. In addition, the B–O–B bridged complexes featured a helical structure formed through the hybridization of one B–O–B and two BF<sub>2</sub> moieties (Fig. 3a). X-ray crystallography analysis revealed distinct nonplanar geometries critical for their chiroptical properties. The optically resolved (P)/(M)-enantiomers yielded enantiopure forms with CD signals of  $g_{\text{abs}}$  reaching 0.012 and CPL activity with a  $g_{\text{lum}}$  reaching  $10^{-3}$  in both solution and polymer films. The dimethylaminobenzene-modified B–O–B bridged complex demonstrated an OFF/ON fluorescence and CPL responses upon protonation, emphasizing its potential as a chiroptical sensor (Fig. 3c–e). This work represents a significant advancement in helically chiral multinuclear boron materials. By integrating innovative molecular design, synthetic versatility, and extensive computational and experimental analyses, it lays the groundwork for the development of efficient optical sensors and chiral emitters. The simultaneous discovery of these complementary structures with distinct chiral properties exemplifies a novel approach to material design in the field of luminescent multinuclear boron complexes.

## Dinuclear triple-helical complexes and their chiroptical properties

Inspired by the natural helical structures found in DNA and polysaccharides, the synthesis of helical complexes using multidentate ligands and transition metals has been extensively explored. These helicates have a long history, with early examples focusing on a variety of ligand–metal combinations.<sup>31</sup> The previous section highlighted the active research on chiral multinuclear boron complexes. Beyond boron-based systems, studies on luminescent main-group metal complexes have garnered increasing interest.<sup>32,33</sup> In response to this trend, luminescent complexes based on group 13 elements, including aluminum, gallium, and indium, have attracted significant attention due to their potential for structural and functional versatility. This section explored the synthesis of such complexes, the role of multidentate ligands in inducing helical chirality, and their chiroptical and photophysical properties.

Aluminum (Al) luminescent complexes are particularly attractive due to the element's abundance ( $\approx 8\%$  in the Earth's crust) and low cost, with several examples documented in the literature.<sup>34–36</sup> However, stable chiral Al complexes remain underexplored, despite some reports on dinuclear double- and triple-stranded helicates containing rare-earth metals. With these challenges in mind, efforts have focused on developing novel Al complexes with intense luminescence and stable chiroptical properties. In 2021, a family of helically chiral Al complexes adopting a dinuclear triple-stranded helicate structure was developed by reacting tetradentate Schiff base ligands with



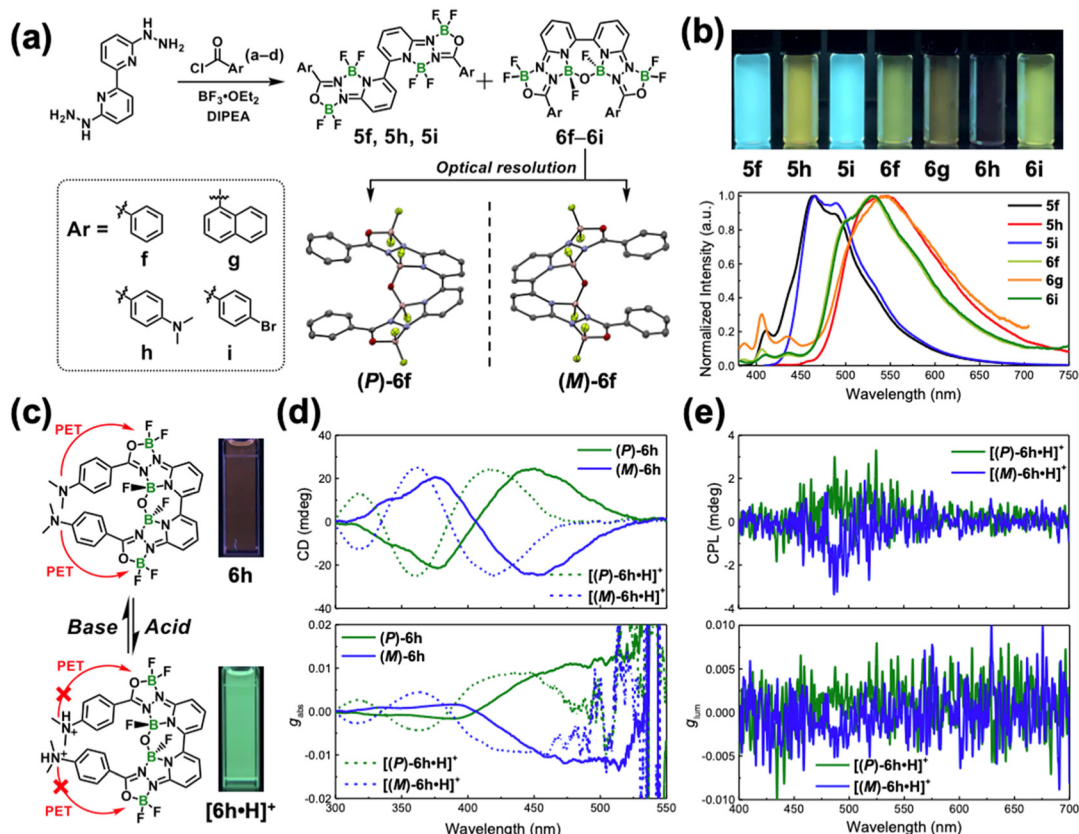


**Fig. 3** (a) Simultaneous synthesis of multinuclear boron complexes with tetra-BF<sub>2</sub> (5) and B–O–B bridged (6) configurations. X-ray single crystal structure of 6f is also shown, with ellipsoids set at 50% probability. (b) Photographs and fluorescence spectra of tetra-BF<sub>2</sub> and B–O–B bridged complexes in toluene. (c) Structures and fluorescence change of complex 6h upon protonation/deprotonation. PET: photoinduced electron transfer. Chiroptical properties of (d) CD and  $g_{abs}$ , (e) CPL and  $g_{lum}$  spectra of 6h enantiomers in toluene upon protonation. Reproduced with permission from ref. 16 copyright (2024) Royal Society of Chemistry.

aluminum chloride (Fig. 4a and b). X-ray crystal analysis confirmed the helical conformation and the existence of (P)- and (M)-enantiomers (Fig. 4c). These complexes exhibited fluorescence ranging from cyan to orange, depending on the ligand substituents (Fig. 4d).<sup>37</sup> Racemic Al complexes were optically resolved to achieve enantiopure forms with chiroptical properties. The enantiopure (P)- and (M)-enantiomers displayed multicolored CPLs (cyan, yellow, and orange) with moderate  $g_{lum}$  in the  $10^{-3}$  range (Fig. 4f). A white CPL response was achieved by mixing enantiomers with cyan- and yellow-emissive enantiopure complexes (Fig. 4g). DFT and TD-DFT calculations provided insights into the influence of helical chirality on electronic transitions, correlating structural twists with luminescence properties. This work demonstrates the potential of these dinuclear triple-stranded Al helicates in creating multicolor CPL materials and white-light emissive systems through enantiomeric combinations.

Building on the findings from Al-based helicates, the potential of helical complexes containing dinuclear gallium and indium metal ions was further investigated (Fig. 4a and b).<sup>38</sup> These dinuclear triple-stranded helical complexes,

formed using a simple bisiminopyrrole tetradeятate ligand and metal ions, revealed new dimensions of the structural and optical properties within this family. Optical resolution achieved enantiopure forms with enhanced stability across solvents and temperatures. This work highlights the importance of metal variation in modulating CPL properties, making these helicates versatile for applications ranging from optical sensing to advanced display technologies. Moreover, it bridges the gap between different group 13 elements, paving the way for further exploration of metal-ligand interactions.

To explore the substituent effects in dinuclear triple-helical complexes on chiroptical performance, deepening the understanding of the structure–property relationship is essential. In 2024, the effects of substituent modifications on the optical and chiroptical properties of dinuclear triple-stranded Al helicates were systematically evaluated (Fig. 4d).<sup>39</sup> Introducing methyl and ethyl groups to specific ligand sites altered the torsional angles and structural relaxation in the excited state, leading to shifts in absorption and emission wavelengths. These structural adjustments, confirmed *via* X-ray crystallography and supported by DFT, resulted in notable Stokes shifts

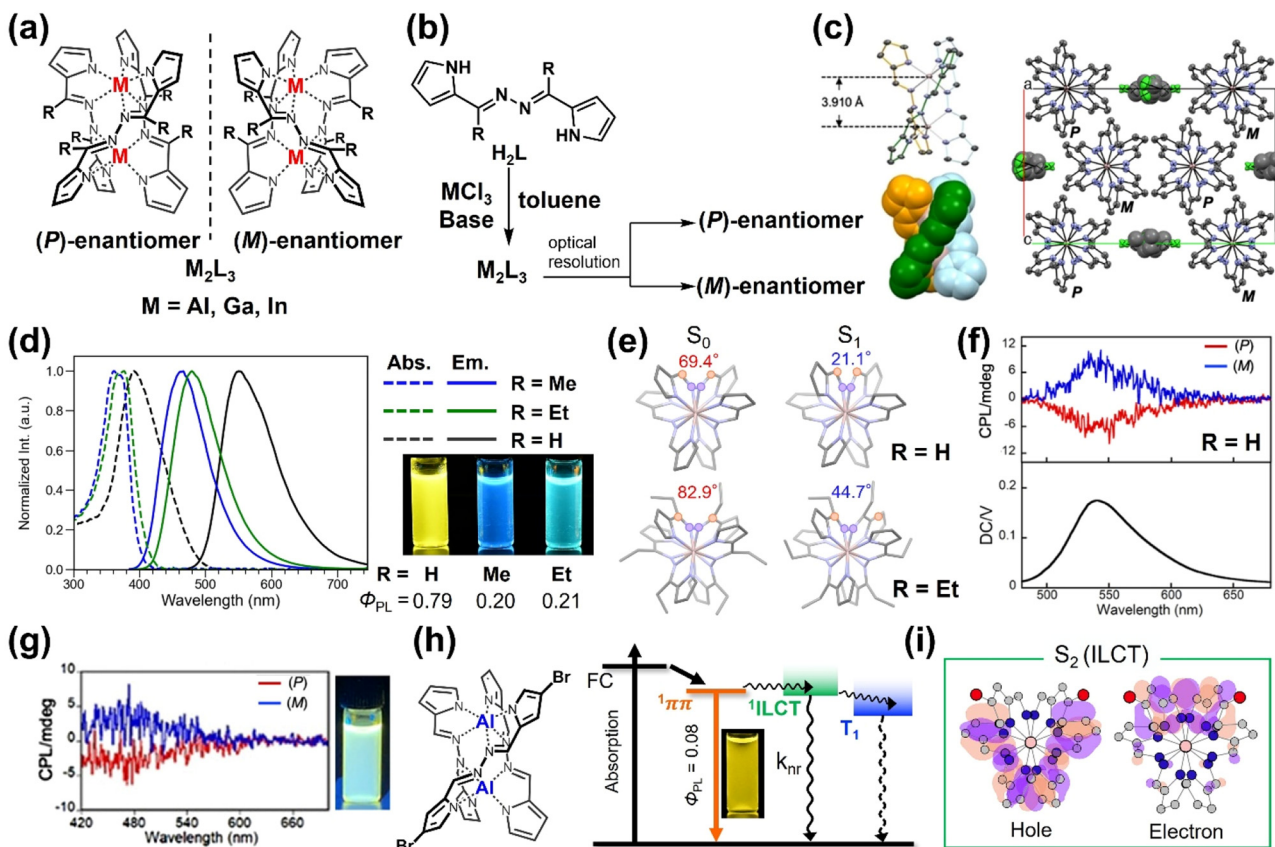


**Fig. 4** (a) Dinuclear triple-stranded helicates with Group 13 elements, showing (P)- and (M)-enantiomers. Reproduced with permission from ref. 37 copyright (2021) Wiley, ref. 38 copyright (2021) The Chemical Society of Japan, and ref. 39 copyright (2024) American Chemical Society. (b) Synthesis of Al, Ga, In-based helicates and optical resolution of (P)- and (M)-forms. Reproduced with permission from ref. 37 copyright (2021) Wiley, ref. 38 copyright (2021) The Chemical Society of Japan, and ref. 39 copyright (2024) American Chemical Society. (c) Single-crystal structure of the aluminum helicate ( $R = H$ ), (P)-form was shown. Ellipsoids are set at 50% probability. Reproduced with permission from ref. 37 copyright (2021) Wiley. (d) Absorption and emission spectra of Al helicates ( $R = H$ , Me, Et) in toluene with the photographs under ultraviolet light. Reproduced with permission from ref. 39 copyright (2024) American Chemical Society. (e) Dihedral angles for Al complexes ( $R = H$ , Et) in  $S_0$  and  $S_1$  states, showing structural relaxation and large Stokes shift. Reproduced with permission from ref. 39 copyright (2024) American Chemical Society. (f) CPL and DC spectra of Al complex ( $R = H$ ) in  $CH_2Cl_2$ . Reproduced with permission from ref. 37 copyright (2021) Wiley. (g) White CPL from mixed Al helicates when substituents are H and Me. Reproduced with permission from ref. 37 copyright (2021) Wiley. (h) Energy diagram for the heteroleptic complex, showing decreased quantum yield due to ILCT. Reproduced with permission from ref. 40 copyright (2024) American Chemical Society. (i) Natural transition orbitals of holes and electrons in the  $S_2$  electronic states at the  $S_1$  optimized structure. Reproduced with permission from ref. 40 copyright (2024) American Chemical Society.

and high photoluminescence quantum yields (Fig. 4e). Optical resolution provided enantiomers with distinct CPL signatures, advancing their applicability in security inks and optoelectronics. This study underscores the importance of precise ligand design in tuning material properties, offering valuable principles for future functional dye design.

Most recently, brominated Schiff base ligands were utilized to develop homoleptic and heteroleptic dinuclear triple-stranded Al helicates, where the degree of bromination modulated inter-ligand charge transfer (ILCT) states, enabling emission tunability from yellow to orange (Fig. 4h).<sup>40</sup> Significant CD and CPL responses were achieved following optical resolution, and ultrafast spectroscopy elucidated ILCT dynamics. Heteroleptic complexes, where one or two ligands were modified by bromine atoms, exhibited

enhanced nonradiative decay and intersystem crossing rates, highlighting their potential as photofunctional materials (Fig. 4i). This research establishes a framework for leveraging ILCT mechanisms to achieve advanced functionalities in Al-based helicates.

These studies collectively emphasize innovations in molecular design, synthesis, and computational understanding of chiral helicates. By integrating diverse metal centers, ligand modifications, and ILCT mechanisms, we established pathways for tunable CPL materials with applications in bioimaging, 3D displays, and secure communications have been established. Future work will focus on extending these principles to other metal-ligand systems and exploring their integration into device architectures for sustainable photonics.



## Conclusions and outlook

Recent advancements in the synthesis of multinuclear main-group element complexes, particularly those incorporating group 13 elements, along with the development of materials with chiral optical properties, have been highlighted in this study. By employing coordination chemistry, which integrates multidentate ligands with multiple elements, multinuclear main-group element complexes exhibiting both axial and helical chirality have been successfully synthesized. Special emphasis have been placed on their circularly polarized luminescence (CPL) properties. Notably, helical aluminum-based complexes, characterized by their strong luminescent properties and exceptional thermal stability, hold promise as key components for next-generation light-emitting devices.

Despite the significant progress in the design and synthesis of chiral multinuclear main-group element complexes, several challenges remain. In particular, improving long-term stability, solubility, and cost-efficiency are critical areas requiring for further development. The integration of machine learning and artificial intelligence into material discovery is expected to accelerate the identification of new chiral complexes with tailored properties.<sup>41</sup> However, serendipitous discoveries of novel chiral complexes will remain essential, driven by the accumulation of numerous synthetic experiments. The continued relevance of compounds such as BODIPY, developed in 1968 and still a cornerstone in modern research, including our own work,<sup>42–44</sup> underscores the importance of exploring related compounds and derivatives.<sup>45,46</sup> Scale-up synthesis remains crucial to make these complexes practical and commercially viable, and future research will play role in overcoming these challenges.

## Author contributions

T. O. wrote the manuscript in consultation with Y. O.

## Data availability

No primary research results, software or code have been included and no new data were generated or analyzed as part of this frontier.

## Conflicts of interest

There are no conflicts to declare.

## Acknowledgements

This work was supported by JSPS KAKENHI Grant Number JP24K01471 and JP22H02123. We also thank Dr Luxia Cui at the Graduate School of Engineering, Kyushu University for English editing.

## References

- S. R. LaPlante, L. D. Fader, K. R. Fandrick, D. R. Fandrick, O. Hucke, R. Kemper, S. P. F. Miller and P. J. Edwards, *J. Med. Chem.*, 2011, **54**, 7005–7022.
- F. Pop, N. Zigon and N. Avarvari, *Chem. Rev.*, 2019, **119**, 8435–8478.
- E. Yashima, N. Ousaka, D. Taura, K. Shimomura, T. Ikai and K. Maeda, *Chem. Rev.*, 2016, **116**, 13752–13990.
- B. P. Bloom, Y. Paltiel, R. Naaman and D. H. Waldeck, *Chem. Rev.*, 2024, **124**, 1950–1991.
- I.-S. Tamgho, A. Hasheminasab, J. T. Engle, V. N. Nemykin and C. J. Ziegler, *J. Am. Chem. Soc.*, 2014, **136**, 5623–5626.
- C. Yu, Z. Huang, X. Wang, W. Miao, Q. Wu, W.-Y. Wong, E. Hao, Y. Xiao and L. Jiao, *Org. Lett.*, 2018, **20**, 4462–4466.
- S. P. Parambil, F. D. Jong, K. Veys, J. Huang, S. P. Veettil, D. Verhaeghe, L. V. Meervelt, D. Escudero, M. V. D. Auweraer and W. Dehaen, *Chem. Commun.*, 2020, **56**, 5791–5794.
- C. Yu, X. Fang, H. Wang, X. Guo, L. Sun, Q. Wu, L. Jiao and E. Hao, *J. Org. Chem.*, 2021, **86**, 11492–11501.
- E. Hao, C. Yu, Y. Sun and L. Jiao, *Synlett*, 2024, 37–54.
- S. Sultan, L. Crovetto and R. Rios, *Chem. Commun.*, 2025, **61**, 1989–2010.
- H. Lu, J. Mack, T. Nyokong, N. Kobayashi and Z. Shen, *Coord. Chem. Rev.*, 2016, **318**, 1–15.
- M. Ihara, L. Cui, Y. Konishi, Y. Hisaeda and T. Ono, *Chem. Lett.*, 2022, **51**, 300–302.
- L. Cui, H. Shinjo, T. Ichiki, K. Deyama, T. Harada, K. Ishibashi, T. Ehara, K. Miyata, K. Onda, Y. Hisaeda and T. Ono, *Angew. Chem., Int. Ed.*, 2022, **61**, e202204358.
- L. Cui, M. Maeda, Y. Hisaeda and T. Ono, *J. Phys. Chem. C*, 2022, **126**, 18152–18158.
- L. Cui, K. Deyama, T. Ichiki, Y. Konishi, A. Horioka, T. Harada, K. Ishibashi, Y. Hisaeda and T. Ono, *J. Mater. Chem. C*, 2023, **11**, 2574–2581.
- L. Cui, R. Furuta, T. Harada, T. Konta, Y. Hoshino and T. Ono, *Dalton Trans.*, 2024, **53**, 9183–9191.
- T. Ono, *J. Inclusion Phenom. Macrocyclic Chem.*, 2024, DOI: [10.1007/s10847-024-01243-3](https://doi.org/10.1007/s10847-024-01243-3).
- T. Ono, D. Koga, K. Yoza and Y. Hisaeda, *Chem. Commun.*, 2017, **53**, 12258–12261.
- T. Ono, N. Xu, D. Koga, T. Ideo, M. Sugimoto and Y. Hisaeda, *RSC Adv.*, 2018, **8**, 39269–39273.
- T. Ono, H. Shinjo, D. Koga and Y. Hisaeda, *Eur. J. Org. Chem.*, 2019, 7578–7583.
- D. Koga, T. Ono, H. Shinjo and Y. Hisaeda, *J. Phys. Chem. Lett.*, 2021, **12**, 10429–10436.
- A. Nowak-Król, P. T. Geppert and K. R. Naveen, *Chem. Sci.*, 2024, **15**, 7408–7440.
- Y. Xu, Z. Ni, Y. Xiao, Z. Chen, S. Wang, L. Gai, Y.-X. Zheng, Z. Shen, H. Lu and Z. Guo, *Angew. Chem., Int. Ed.*, 2023, **62**, e202218023.
- Z. Chen, Z. Ni, X. Y. Chen, Y. Xu, C. Yu, S. Wang, X. Y. Wang and H. Lu, *Aggregate*, 2024, **5**, e498.



25 M. Bröring, F. Brégier, R. Krüger and C. Kleeberg, *Eur. J. Inorg. Chem.*, 2008, **2008**, 5505–5512.

26 P. J. Brothers, *Chem. Commun.*, 2008, 2090–2102.

27 A. C. Y. Tay, B. J. Frogley, D. C. Ware, J. Conradi, A. Ghosh and P. J. Brothers, *Angew. Chem., Int. Ed.*, 2019, **58**, 3057–3061.

28 N. Xu, T. Ono, Y. Morita, T. Komatsu and Y. Hisaeda, *Inorg. Chem.*, 2021, **60**, 574–583.

29 S. Wang, Z. Wang, W. Song, H. Gao, F. Wu, Y. Zhao, K. S. Chan and Z. Shen, *Dalton Trans.*, 2022, **51**, 2708–2714.

30 T. Mori, *Chem. Rev.*, 2021, **121**, 2373–2412.

31 C. Piguet, G. Bernardinelli and G. Hopfgartner, *Chem. Rev.*, 1997, **97**, 2005–2062.

32 Y. Aoyama, Y. Sakai, S. Ito and K. Tanaka, *Chem. – Eur. J.*, 2023, **29**, e202300654.

33 V. S. Thoi, J. R. Stork, D. Magde and S. M. Cohen, *Inorg. Chem.*, 2006, **45**, 10688–10697.

34 C. Ikeda, S. Ueda and T. Nabeshima, *Chem. Commun.*, 2009, 2544–2546, DOI: [10.1039/b820141b](https://doi.org/10.1039/b820141b).

35 F. L. Portwich, Y. Carstensen, A. Dasgupta, S. Kupfer, R. Wyrwa, H. Görls, C. Eggeling, B. Dietzek, S. Gräfe, M. Wächtler and R. Kretschmer, *Angew. Chem., Int. Ed.*, 2022, **61**, e202117499.

36 J.-W. Wang, F. Ma, T. Jin, P. He, Z.-M. Luo, S. Kupfer, M. Karnahl, F. Zhao, Z. Xu, T. Jin, T. Lian, Y.-L. Huang, L. Jiang, L.-Z. Fu, G. Ouyang and X.-Y. Yi, *J. Am. Chem. Soc.*, 2023, **145**, 676–688.

37 T. Ono, K. Ishihama, A. Taema, T. Harada, K. Furusho, M. Hasegawa, Y. Nojima, M. Abe and Y. Hisaeda, *Angew. Chem., Int. Ed.*, 2021, **60**, 2614–2618.

38 K. Ishihama, T. Ono, T. Okawara, T. Harada, K. Furusho, M. Hasegawa, Y. Nojima, T. Koide, M. Abe and Y. Hisaeda, *Bull. Chem. Soc. Jpn.*, 2021, **94**, 573–578.

39 K. Ueno, Y. Konishi, L. Cui, T. Harada, K. Ishibashi, T. Konta, A. Muranaka, Y. Hisaeda, Y. Hoshino and T. Ono, *Inorg. Chem.*, 2024, **63**, 6296–6304.

40 Y. Konishi, T. Ehara, L. Cui, K. Ueno, Y. Ishigaki, T. Harada, T. Konta, K. Onda, Y. Hoshino, K. Miyata and T. Ono, *Inorg. Chem.*, 2024, **63**, 11716–11725.

41 M. Sumita, K. Terayama, N. Suzuki, S. Ishihara, R. Tamura, M. K. Chahal, D. T. Payne, K. Yoshizoe and K. Tsuda, *Sci. Adv.*, 2022, **8**, eabj3906.

42 S. Tsumura, K. Ohira, K. Imato and Y. Ooyama, *RSC Adv.*, 2020, **10**, 33836–33843.

43 D. Jinbo, K. Imato and Y. Ooyama, *RSC Adv.*, 2019, **9**, 15335–15340.

44 S. Tsumura, K. Ohira, K. Hashimoto, K. Imato and Y. Ooyama, *Mater. Chem. Front.*, 2020, **4**, 2762–2771.

45 A. Vyšniauskas, I. López-Duarte, N. Duchemin, T.-T. Vu, Y. Wu, E. M. Budynina, Y. A. Volkova, E. P. Cabrera, D. E. Ramírez-Ornelas and M. K. Kuimova, *Phys. Chem. Chem. Phys.*, 2017, **19**, 25252–25259.

46 P. Kaur and K. Singh, *J. Mater. Chem. C*, 2019, **7**, 11361–11405.

